Discrepant Adversarial Domain Adaptation Network for Rolling Bearing Intelligent Fault Diagnosis under Varying Working Condition

Kai Zheng, *Member, IAENG*, Pengyuan Zhao, Jinfeng Xiong, Yin Bai, Yongying Li, Zihao Long and Zheng Zhang

***Abstract*—In the real industry field application, the signal collected across various working scenarios shows obvious distribution discrepancy. Adversarial domain adaptation networks have been extensively investigated in varying working condition fault diagnosis scenario. However, exist adversarial domain adaptation methods have no regard for the task-specific decision boundaries across domain and the characteristics of the discriminative embedded feature, which may damage the inherent properties of target data distinction and deteriorate the fault diagnosis performance. To resolve these concerns, a discrepant adversarial domain adaptation network (DADAN) is proposed to align embedded features across domains and locate the optimized category decision boundaries simultaneously. Specifically, in the domain-wise level, the double adversarial learning and the domains feature center clustering alignment are combined to facilitate the extraction of the underly distinguishing characteristics across domains. In the class-wise level, the dual distinct classifiers with different structures are designed to obtain the decision boundaries from different perspectives. Utilizing discrepancy measurement strategy of dual different classifiers, the internal structural discriminative information of target domain instances can be captured, which is conducive to achieve better decision boundaries. Two case studies with several transfer tasks under varying working conditions are taken to assess the effectiveness of DADAN. Moreover, the outcomes indicate that DADAN outperforms the leading-edge approaches.**

***Index Terms*—Discrepant adversarial, domain adaptation, Dual classifiers, Feature center alignment, Varying working condition, Fault diagnosis.**

Manuscript received April 26, 2024; revised January 23, 2025.

This research is supported by the National Natural Science Foundation of China (Grant No. 51905065).

Kai Zheng is an associate professor in School of Advanced Manufacturing Engineering, Chongqing University of Posts and Telecommunications, Chongqing 400065, China. (e-mail: zhengkai2001@163.com).

Pengyuan Zhao is a graduate student of Chongqing University of Posts and Telecommunications, Chongqing 400065, China (e-mail: 2478434112@qq.com)

Jinfeng Xiong is a graduate student of Southern University of Science and Technology, Shenzhen 518000, China (e-mail: 2376625828@qq.com)

Yin Bai is a lecturer in School of Advanced Manufacturing Engineering, Chongqing University of Posts and Telecommunications, Chongqing, 400065, China (e-mail: baiyin@cqupt.edu.cn)

Yongying Li is a graduate student of Chongqing University of Posts and Telecommunications, Chongqing 400065, China (e-mail: 1038366117@qq.com)

Zihao Long is a graduate student of Chongqing University of Posts and Telecommunications, Chongqing 400065, China (e-mail: 1656021039 @qq.com)

Zheng Zhang is a PhD student of Wuhan University of Science and Technology, Wuhan 430000, China (zzwustphd@163.com)

I. INTRODUCTION

Rolling bearing is known as "joint" in mechanical systems such as in industry robot, CNC machine and wind turbine, etc. Its working status heavily influences the functionality of the mechanical systems [1-3]. Bearing fault diagnosis is significantly crucial to secure the secure and dependable performance of mechanical system [4-6]. Researchers have come up with a range of intelligent fault diagnosis methods, such as support vector machine. [7], random forest [8] and artificial neural network [9] etc. Lately, the methods of deep learning have emerged as a mainstream approach in bearing fault diagnosis [10-11]. Unlike conventional machine learning approaches, the deep learning methods reveal better classification performance as they can automatically learn depth features [9]. The methods such as convolutional neural network [12], auto-encoder [13], and long short-term memory [14] were investigated for fault diagnosis.

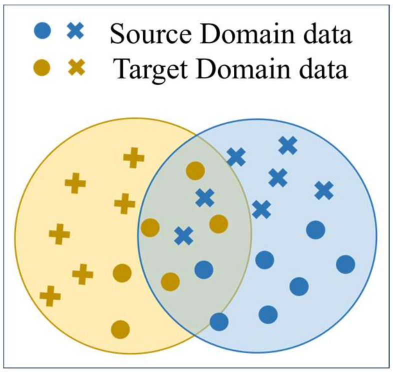

Fig. 1. Domain bias

The above deep learning-based methods gain outstanding performance with sufficient labeled training data and abide by the basic assumption that the attribute distribution between the training and testing samples should be consistent. [15]. Nevertheless, in practical industrial applications, obtaining a sufficient amount of labeled fault data is often impractical. Moreover, due to the various tasks in industrial process, the speed and load of mechanical systems are variable [16]. Consequently, there is always distributional difference between the source and target training data, as illustrated in Fig.1. As a result, the above deep learning methods will perform poorly or even not work when face the fault diagnosis tasks with variable working conditions. Hence, it is critically essential to explore fault diagnosis frameworks incorporating domain adaptation capabilities to achieve precise fault identification in unlabeled target domains.

Domain adaptation serves as a representative approach within the realm of transfer learning, which learns hidden representation from source domain with numerous labeled samples and then adapt to target domain with unlabeled samples. Due to superiority of domain adaptation method for addressing domain transfer problems, it has been embedded in deep learning framework for mechanical system fault diagnosis.

At present, there are two main kinds of approaches which embed domain adaptation into deep network frameworks for fault diagnosis. The first type is called statistical discrepancy-based methods, which seek to minimize statistical discrepancy between feature distributions. The very popular methods include maximum mean discrepancy (MMD) [19] and its improvement methods such as MK-MMD [20] and CORAL [21-22]. In the MMD approach, a loss function is designed based on feature distribution to minimize domain bias between source and target domain. The second approach is termed as an adversarial-based method, which leverages a two-player minimax game combined with adversarial optimization to align feature distributions of source and target domains. The first player is trained to maximize the differentiation between the two, while the other one is designed to identify the features that remain consistent across domains [23]. The distance of embedded feature distribution in the source and target domain is continuously reduced in confrontation between the two architectures. Given the outstanding performance of adversarial-based methods, they arouse close attention from researchers. Han, T. et al. [24] developed a deep adversarial convolutional neural network (DACNN) method for bearing fault diagnosis. It added an additional discriminative classifier, which was designed to refine the convolutional blocks using partitioned data subsets. Chai, Z et al. [25] introduced a fine-grained adversarial network (FANDA) method for domain adaptation. FANDA employed competition against multiple-domain discriminators to learn features, attaining comprehensive alignment between the two domains, along with precise alignment for each specific fault category. Li, F. et al. [26] introduced a deep convolution domain-adversarial transfer learning (DCDATL) approach for rolling bearing fault diagnosis. In this approach, a deep convolutional residual network was designed to extract high-level feature representations. Additionally, domain adversarial training was implemented by leveraging the joint distribution of labeled instances from the source domain and unlabeled samples from target domain. Qin, Y. et al. [27] introduced a parameter sharing adversarial domain adaptation network (PSADAN). To streamline the network architecture, the proposed approach introduces an integrated classification module that merges the functionalities of fault identification and domain discrimination into a single framework. Additionally, the CORAL loss was incorporated into the adversarial process to enhance domain alignment.

It should be noted that the above adversarial network-based fault diagnosis methods mainly seek to align the feature boundaries of dataset across domain. The efficacy of these methods heavily depends on the precision of source classifiers. However, the collected samples are frequently affected by noise and large random impulses [2-3]. The vibration signal features of the two differ, indicating that one may have unique category boundaries.

Consequently, the performance will significantly degrade when the domain discrepancy becomes substantial. Therefore, it is necessary to consider the unique classification boundaries across domain for adaptation. Saito et.al [28] presented a new network framework which uses two classifiers to compete with each other to gain the task specific boundaries of the target domain, Wu et al [29] developed a adversarial optimization to maximize inter-classifier divergence, effectively aligning feature representations across distinct data domains through a discriminative feature integration strategy. Jiao et.al [30] introduced a double-level adversarial domain adaptation network (DL-ADAN). The DL-ADAN architecture comprises a deep convolutional network-based feature extractor, a domain discriminator, and two label classifiers. Through the use of two minimax adversarial processes, DL-ADAN achieved remarkable performance for fault diagnosis. However, the above methods still confront several limitations, as outlined below. Firstly, the structure of the two classifiers is the same, which will generate similar classification boundaries. However, in the industry application, due to heavy background noise, the actual vibration signal of rolling bearings with different fault categories may exhibit a very similar characteristic. In this case, the fault pattern in the high dimension embedded space may be very close or even overlap to each other. The ideal classification boundaries may not be obtained for fault detection using the two same classifiers, as demonstrated in Fig.2. Moreover, the embedded feature structural similarity of same fault category between the two domains may not been fully aligned in the latent embedded space, which will hinder the performance of fault classification.

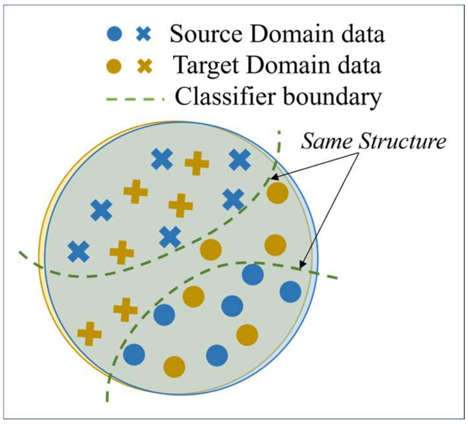

Fig. 2. Domain adaptation based on dual classifiers with same structure

Aiming at above limitations, a new DADAN is proposed. In the domain-wise level, the DADAN algorithm pursues to obtain the domain invariant feature through simultaneously adversarial learning. In the class-wise level, two classifiers with different structures are designed to compete against with the feature extractor for detecting and discriminating the ambiguous features near class boundaries. Moreover, consider the feature structural similarity of the same fault category across domains, the feature center alignment is employed to mitigate the effect of cross-domain mismatching, as demonstrated in Fig.3. To sum up, the proposed network not only considers the task-specific decision boundaries across domains but also pays attention of feature similarity of same fault category across domains, thus solves the issue of misclassification of target domain samples when the domain gap is over large. Furthermore, the dataset collected from two test rigs serves to assess the performance of proposed DADAN approach in bearing fault detection. Finally, five advanced approaches are utilized for comparative analysis. Experimental results reveal that the DADAN significantly outperforms existing solutions in diagnosing bearing defects across diverse operating scenarios.

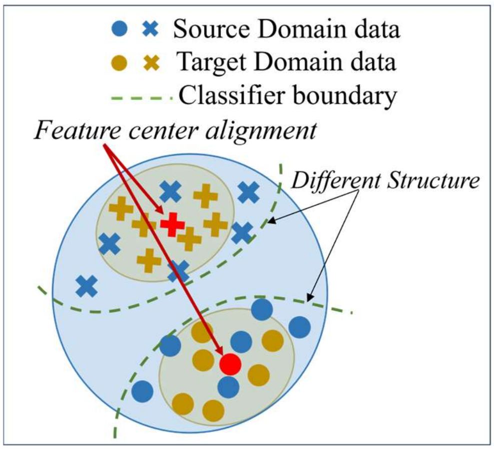

Fig. 3. Domain adaptation based on dual classifiers with different structures

The contributions of this paper are summarized as follows:

(1) A novel DADAN approach is introduced for bearing fault detection. This method aims to align domain-wise level and class-wise level adaptations to achieve effective cross-domain fault identification.

(2) The dual task-specific classifiers are designed to establish task-specific decision boundaries within the target domain. Improved decision boundaries in target domain are achieved through the employment of dual classifiers.

(3) The feature center alignment across domains is proposed to facilitate extraction of domain-invariant features and alignment of class-level between domains.

(4) Two trials are performed to evaluate the efficacy of DADAN. Furthermore, five advanced approaches are compared to prove the superiority of DADAN.

The rest part of this paper is arranged as described below: Section 2 provides the foundational theory. Section 3 thoroughly explains the DADAN. In Section 4, two evaluations are performed to validate performance of DADAN. Section 5 presents the concluding remarks.

II. Proposed Method

A. Problem definition

In the industry application, the mechanical system often works in varying working condition. For example, the speed and load of industry robot end operators are always changing when conducting a range of tasks in the automation assembly workshop. Therefore, the discrepancy in distribution between the training and testing samples exhibits a significant divergence. Domain adaptation becomes the mainstream approach for resolving this difficulty. Given a source domain containing labeled sample, $D_S=\{X_S,Y_S\}=\{(x_S^i,y_S^i)\}_{i=1}^{n_s}$ which contains n_s labeled samples, also with a target domain $D_t=\{X_t,Y_t\}=\{(x_t^j,y_t^j)\}_{j=1}^{n_t}$ with n_t unlabeled samples, the spread of the source and target domain can be represented as $P_s(x_s)$ and $P_t(x_t)$. It should be noting that the $P_s(x_s)\neq P_t(x_t)$ for a fault detection across domains task. The main goal for domain adaptation fault diagnosis task is to design a new algorithm, which can discover a shared common latent space between the source and target domains, allowing the target samples to be classified under the supervision of the source domain.

B. The framework of DADAN

The architecture of DADAN is illustrated in Fig. 4. The DADAN considers the class-specific decision boundaries for classification across different classes. which has better performance for dealing with the cross-domain adaptation problem. DADAN has a feature extractor F , a domain discriminator D and the dual classifier C_1 and C_2 .The feature generator F and the discriminator D engage in adversarial learning to extract domain-invariant features between source and target domains. Note that the dual classifier C_1 and C_2 has different structure for obtaining better classification boundaries from different perspective. The classifier C_1 is a dense neural network classifier while C_2 is prototype classifier. The two classifiers with different structures are capable of precisely distinguishing the target samples that are distinct from source samples. Meanwhile, the feature center alignment loss is added to align source and target sample center to obtain better prediction result. Detailed introduction of DADAN is illustrated in following sections.

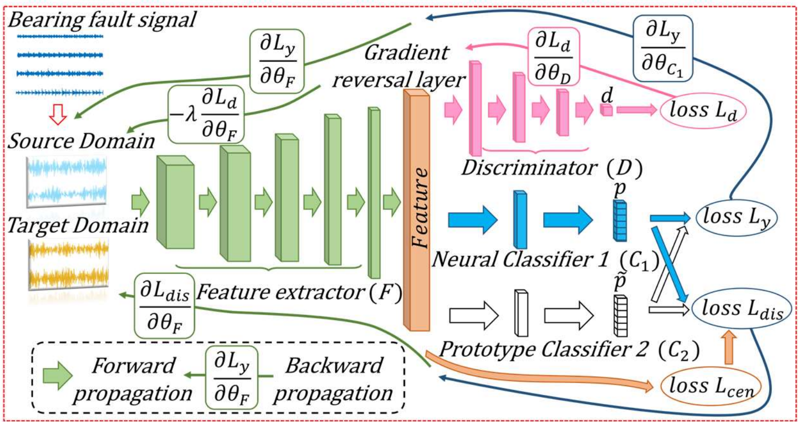

Fig.4 The proposed DADAN intelligent diagnostic framework

C. The dual classifier with different properties

Inspired by Prototypical Networks [31] and adversarial dual classifiers [32], we utilize two classifiers to extract and represent the latent discriminative features from different viewpoints. The dual classifier can obtain different prediction results to identify the target sample beyond the scope of source supervision. Specifically, C_1 is conventional multi-layer nonlinear classifier, which can be called fully connected neural classifier. The classifier C_1 is defined as:

$$C_{1,p} = \left\{ p_{i,k} \right\}_{k=1}^{K} = softmax\left(C_1\left(F(x_i) \right) \right) \tag{1}$$

Moreover, we design the classifier C_2 based on clustering characteristics in embedded feature space, which have no trainable parameters. The classifier can enhance the latent target discrimination information through discriminative clustering in the feature space Z, which can automatically give the predication probability with input signal in embedded feature space Z. For the instance feature $z_i = F(x_i)$, the predication probability vector $\tilde{p}_{i,k}$ of soft cluster assignments can be obtained as follows [31, 33]:

$$\tilde{p}_{i,k} = \frac{\varepsilon + \exp(-\| z_i - \mu_k \|_2)}{\sum_{k'=1}^{K} (\varepsilon + \exp(-\| z_i - \mu_{k'} \|_2))} \tag{2}$$

where μ_k is learnable embedded feature centers of both source and target samples in embedded space, ε is protection parameter which can avoid that the denominator becomes zero. The predication probability of classifier C_2 is depicted as:

$$C_{2,\tilde{p}} = \{ \tilde{p}_{i,k} \}_{k=1}^{K} \tag{3}$$

The embedded feature centers of the two domains are calculated as follows:

$$u_k = \frac{\sum_{i=1}^{n} p_{i,k} z_i}{\sum_{i=1}^{n} p_{i,k}} \tag{4}$$

More specifically, p is the predication probability gained by the trainable network classifier C_1 .It is noteworthy that $p_{i,k} = y_{i,k}$ when calculating the cluster feature center of source domain, where $y_i = \left\{ y_{i,k} \right\}_{k=1}^{K}$ is true label of samples.

D. Domain boundaries alignment

Similar to the Domain-Adversarial Training of Neural Networks (DANN) [23], discriminator D should distinguish the feature extracted by feature extractor F from source and target domain, while F aims to effectively deceive discriminator D. Meanwhile, feature extractor F and trainable classifier C_1 need to reduce classification error rate of source domain sample as much as possible. Hence, the constructed network can simultaneously align the domain feature boundary while obtaining the accurate classifier on source domain. At this phase, the objective loss function contains prediction loss and domain loss, which can be formulated as:

$$F_d(\theta_F, \theta_c, \theta_D) = \frac{1}{n_s} \sum_{x_i \in D_s} [L_c(C_{1,p}, y_i) + L_c(C_{2,\tilde{p}}, y_i)]$$
$$- \frac{1}{n_s + n_t} \sum_{x_i \in D_s \cup D_t} L_d(D(F(x_i)), d_i) \tag{5}$$

where L_c denotes the cross-entropy loss for two classifiers and L_d is binary cross entropy (BCE) loss for the discriminator. y_i is a true label of samples and d_i represents the domain label. Specifically, L_d is expressed as follows:

$$L_d(D(F(x_i)), d_i) = -d_i \log(D(F(x_i)))$$
$$-(1-d_i)\log(1-D(F(x_i))) \tag{6}$$

where d_i is defined as follows:

$$d_i = \begin{cases} 0, & x_i \epsilon D_s \\ 1, & x_i \epsilon D_t \end{cases} \tag{7}$$

E. Classification boundaries alignment

Through domain feature boundary alignment, the feature distribution across domains can be adapted. So far, the similarity in the feature distributions across domain are augmented. However, the vibration signal samples collected from different domain have the unique classification boundaries. Naturally, it is extremely important to exploit the tasks-specific boundaries alignment for accurate machinal fault diagnosis and prediction. Therefore, we devise a new strategy to align the classification boundaries while detecting target samples near decision boundaries using two different labels predict classifiers. In this process, the divergence across the two classifiers is leveraged to recognize target instances that deviate from distribution of source domain. Firstly, we freeze feature extractor F and enhance the divergence given target features. With this operation, the target instances close to the decision boundary are distinguished. Note that classifier C_1 and C_2 have different structures. Therefore, the latent information can be captured from different perspectives. After that, the weights of the dual classifiers are fixed while the feature extractor F is trained to reduce the disparity. During this process, the ambiguous features near decision boundaries can be pushed to the source domain samples which have clear classification boundaries. As a result, the classification boundaries alignment can be achieved. With this process, the different fault categories can be accurately distinguished. Formally, the loss function has the following definition:

$$F_y(\theta_F, \theta_{c_1}, \theta_{c_2}) = \frac{1}{n_s} \sum_{x_i \in D_s} \left[L_c\left(C_{1,p}, y_i \right) + L_c\left(C_{2,\tilde{p}}, y_i \right) \right]$$
$$- \frac{1}{n_t} \sum_{x_i \in D_t} L_{dis}(C_{1,p}, C_{2,p})) \tag{8}$$

The discrepancy loss F_{dis} between the dual classifiers is formulated as:

$$F_{dis}\left(\theta_F, \theta_{c_1}, \theta_{c_2} \right) = \frac{1}{n_t} \sum_{x_t \in D_t} L_{dis}(C_{1,p}, C_{2,\tilde{p}}) \tag{9}$$

where the discrepancy loss is calculated as:

$$L_{dis}\left(C_{1,p}, C_{2,\tilde{p}} \right) = \frac{1}{N} \sum_{i=1}^{N} \left(C_{1,p} - C_{2,\tilde{p}} \right)^2 \tag{10}$$

where L_{dis} denotes the mean square deviation, which serves to evaluate the discrepancy between the two classifiers. Moreover, in the classification boundaries alignment stage, the cluster feature center alignment across domain is employed to obtain better prediction result and convergence performance. The objective loss function is expressed as follows.

$$F_{cen} = L_{cen}(\mu^t, \mu^s) \quad (11)$$

Similarly, the feature center alignment loss can be computed by:

$$L_{cen}(\mu^t, \mu^s) = \frac{1}{N}\sum_{i=1}^{N}(\mu_n^t - \mu_n^s)^2 \quad (12)$$

where μ^t and μ^s represent the feature centroids corresponding to the target instances and the K^{th} category within the embedded feature space, respectively.

III. FAULT DIAGNOSIS OF BEARINGS USING DADAN

A. The trains steps of DADAN

According to the above introduction, the proposed DADAN consists of two boundaries alignment: domain-level boundaries alignment and the class-level boundaries alignment. In domain-level boundaries alignment, the domain feature boundary alignment is obtained via the adversarial interaction between the feature extractor F and the discriminator D. In the class-level boundaries alignment, the dual classifiers with different structures are designed to identify target domain instances that do not conform to the source distribution. Moreover, the loss of cluster centers across source and target domains is incorporated to achieve better classification performance. Specifically, the training process of proposed DADAN is outlined as follows:

Step 1. We conduct training on the feature extractor F and the classifier C_1 within the source domain. Note that the classifier C_2 has no trainable parameters. Naturally, only the weights of the feature extractor F, the classifier C_1 and the discriminator D will be updated. The goal of this step is to optimize a satisfied network for classifying the source domain samples and aligning the domain feature boundary. The objective formulation is expressed as follows:

$$arg\min_{\theta_F,\theta_c} F_d(\theta_F, \theta_c, \theta_D) \quad (13)$$

and

$$arg\max_{\theta_D} F_d(\theta_F, \theta_c, \theta_D) \quad (14)$$

Step 2. On the premise of ensuring the good ability of classifying the source domain samples, we optimize the dual discrepant classifiers by enhancing the distribution divergence between them over target domain instances. In this phase, the feature extractor F remains unchanged, while the classifier C_1 undergoes weight updates. Similarly, the classifier C_2 has no trainable parameters. The goal of this step is to identify target domain instances that deviate significantly from the source domain samples. The training optimization objective function is:

$$arg\min_{\theta_c} F_y(\theta_F, \theta_c, \theta_D) \quad (15)$$

Step 3. To align the classifier boundary between the two kinds of domains, we minimize the divergence in distributions captured by the dual classifiers on the target domain. In this process, we keep the weights of classifier C_1 while optimizing the parameters of feature extractor F. Meanwhile, we minimize the cluster centers of source and target sample. Therefore, the feature extractor tends to make the features of both domains more similar. The objective function is:

$$arg\min_{\theta_F}\left\{F_{dis}\left(\theta_F, \theta_{c_1}, \theta_{c_2}\right) + L_{cen}(\mu^t, \mu^s)\right\} \quad (16)$$

The pseudocode for the training procedure of DADAN is presented below:

Algorithm 1 Training process of the DADAN method

Input: labeled source domain data $D_s = \{X_s, Y_s\} = \left\{\left(x_s^i, y_s^i\right)\right\}_{i=1}^{n_s}$, unlabeled target domain data $D_t = \{X_t\} = \{x_t^j\}_{j=1}^{n_s}$

1: Randomly initialized network F, D and C_1
2: for epoch in epochs do:
3: Compute the center of source data feature and target data feature according to Eq. (4)
4: for batch in batches do:
5: Sample batch $\{(x_s^i, y_s^i)\}_{i=1}^{b}$ and $\{x_t^j\}_{i=1}^{b}$ from D_s and D_t
6: Train F, C_1, D according to Eq. (13) and Eq. (14)
7: Train C_1 according to Eq. (15)
8: end for
9: Train F according to Eq. (16)
10: end for
11: until reach maximum iterations or convergence

B. The fault diagnosis procedures using DADAN

The overall structure of the bearing fault detection identification utilizing DADAN is illustrated in Fig. 5. Key steps of the process are outlined below:

Step 1: The oscillation data from the bearing are gathered using the piezoelectricity acceleration sensors and DAQ card.

Step 2: Based on the segmentation and normalization technique, the signals are equally split into the samples. The processed samples are categorized into the training set, the validation set and the testing set.

Step 3: The samples collected in various operating conditions are set as source and target domain. Then the samples are fed into DADAN.

Step 4: Finally, the health condition of the unlabeled vibration signals of the bearing in varying working conditions is predicated by DADAN.

IV. EXPERIMENTS AND ANALYSIS

We utilize two datasets to assess the effectiveness of DADAN. The first bearing fault dataset is sourced from the open database of Case Western Reserve University (CWRU) diagnostic platform [34]. The second dataset is gathered from the platform that we designed. Regarding the computational aspect, all analyses are carried out on a computer featuring a Core Intel i7-6700 CPU and two Nvidia GTX-2080 GPU. This setup provides the necessary computational power to handle the complex computations involved in validating DADAN. Also, we compare DADAN with five mainstream methods. All the tested methods are implemented using the TensorFlow. The classification accuracy, confusion matrix, convergence performance, t-distributed stochastic neighbor embedding (t-SNE) [35] and kernel density estimation [36] are applied to showcase the performance of all approaches.

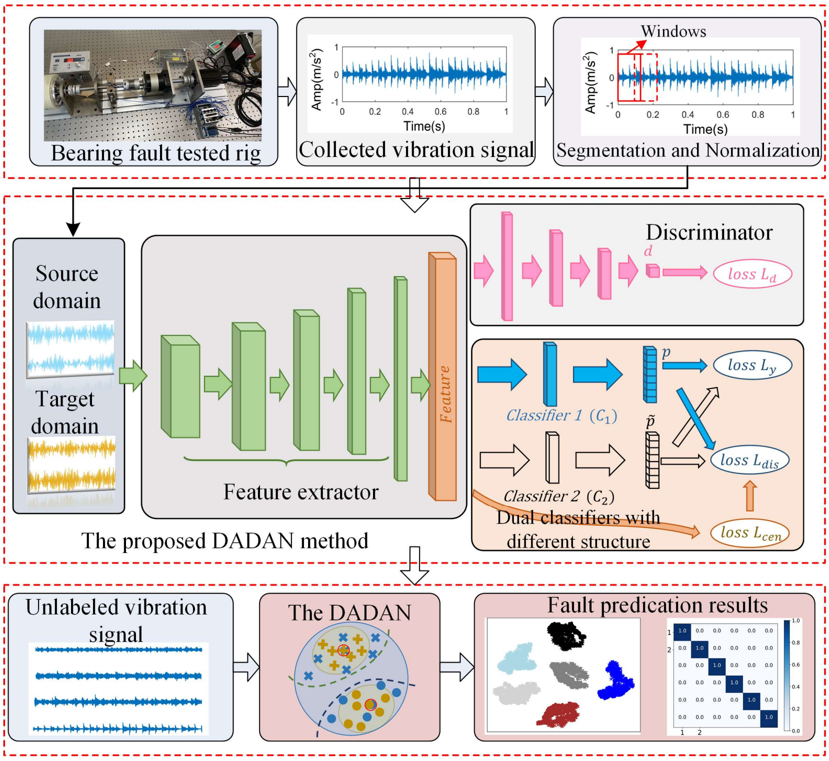

Fig. 5. The fault diagnosis procedures utilizing the proposed DADAN

A. *Implement details*

During the implement process, the 1D CNN serves as feature extractor. The main parameters are illustrated in TABLE I, where operations of convolution and max pooling are denoted as Conv1D and Pool. Moreover, Padding refers to the zero-padding operation. BN denotes batch normalization, while ReLU signifies the rectified linear unit. Learning rate is set to its default value. The training process for DADAN is presented in algorithm 1, where the epoch is set to 300, the ratio of training data in source to target domain is set as 1:1. Moreover, without loss of generality, the proportion of training data to testing data in target domain is set as 7:3. The random seed is set to i. All the methods are repeated five times to obtain the more objective classification accuracy results.

TABLE I: The structure parameters of the proposed method.

Network	Layer	detail
Feature extractor F	Conv1D 1	Kernel 16x32, Stride 1, Padding, Relu, BN, Max-pool 2, Stride 2
	Conv1D 2	Kernel 32x16, Stride 1, Padding, Relu, BN, Max-pool 2, Stride 2
	Conv1D 3	Kernel 64x5, Stride 1, Padding, Relu, BN, Max-pool 2, Stride 2
	Conv1D 4	Kernel 128x3, Stride 1, Padding, Relu, BN, Max-pool 2, Stride 2
	Fc 5	Neuron 512, BN, Relu, Dropout 0.5
Classifier1 C_1	Fc	Neuron Number of categories
Classifier C_2		\
Discriminator D	Fc1	Neuron 256, Relu, Dropout 0.5
	Fc2	Neuron 128, Leaky-relu, Dropout 0.5
	Fc3	Neuron 2, Leaky-relu

B. *Comparison methods*

To emphasize the benefits of the DADAN approach, we compare it with five widely used deep learning-based methods, including: Convolution neural network (CNN), Convolution neural network based on MMD loss (CNN+MMD) [37-38], Domain adversarial neural network (DANN) [24], Maximum classifier discrepancy for unsupervised domain adaptation (MCD-UDA) [28] and Double-level adversarial domain adaptation network (DL-ADAN) [30].

(1) CNN: The basic architecture of CNN approach has a feature extractor and the classifier. The feature extractor includes four convolutional layers (Conv1-Conv2), four max-pooling layers (Pool1- Pool4) and one fully connected layer FC1. In the process of network training, the source domain is used for training while the target domain is employed for testing. Detailed parameters of the kernel size and the step size for each layer in CNN can be found in TABLE I.

(2) CNN-MMD: MMD is a loss function commonly for quantifying distributional discrepancies across different domains. Within the CNN-MMD framework, cross-domain feature alignment is achieved through the optimization process that reduces the MMD metric between the source and target feature distributions. The final objective function of the CNN-MMD network is combined by the classification loss and the MMD loss [38]. To ensure an equitable evaluation, the architecture and fundamental settings of the CNN, which extracts the latent embedded features in RKHS space, are kept identical to those of the proposed DADAN network. The main parameters of MMD can refer to [20].

(3) DANN: DANN is a prominent transfer learning approach for bearing fault classification [24]. The DANN contains a feature extractor, a domain discriminator and a classifier. The structure of DANN can be found in the Ref. [24]. The front convolutional blocks in CNN are employed as the feature extractor. Similarly, all the configurations and

settings of the feature encoder and domain classifier are configured similarly to those in the proposed method. The classifier is set the same as C_1 in the DADAN.

(4) MCD-UDA: MCD-UDA is a popular adversarial learning network [28]. Different from DANN, the architecture of MCD-UDA is formed by a feature extractor and two identical classifiers. The detailed information of MCD-UDA can be found in [28]. Likewise, the feature extractor is identical to DADAN while the dual classifier is set the same as C_1.

(5) DL-ADAN: DL-ADAN [30] is a network which combines the advantages of DANN and CADAN, which can be regarded as the ablation study of this paper. It shows excellent performance in fault diagnosis experiment. The network contains a feature extractor, a domain discriminator and two classifiers. The dual classifiers have same structure, where the parameters are set the same as C_1 in DADAN. In the same vein, the domain discriminator is set the same as DADAN.

Throughout model training, the objective functions are optimized with the Adam algorithm for a fair comparison. The initial learning rate is assigned to be the default value, while the training epochs are configured to be 300. The batch size is configured as 64, and the proportion of training to testing data in the target domain is maintained at 7:3. All approaches are tested five times. We document the best result from each test when the models are in the convergence state. The average classification accuracy is calculated for comparison.

C. *CWRU bearing fault diagnosis result analysis*

We utilize the dataset from the CWRU to assess the effectiveness of DADAN. Fig. 6 illustrates the structural arrangement of the experimental setup, consisting of a 1.5 kW motor, a torque sensor with an encoder, and a power meter. An acceleration sensor was used to capture vibration data under four distinct load levels: 0 hp, 1 hp, 2 hp, and 3 hp. The data were sampled at a frequency of 12 kHz. Each operational scenario encompasses four categories of bearing signals corresponding to different health conditions: (1) normal (N), (2) outer race fault (ORF), (3) inner race fault (IRF), (4) roller fault (BF).

Each fault category includes three severity levels, characterized by defect diameters of 0.007 inches (S: minor), 0.014 inches (M: moderate), and 0.021 inches (L: severe), respectively. The dataset encompasses 4 operational states, with each state comprising 10 distinct bearing fault classes. The labels of the 10 categories of bearing fault are marked as SBF, MBF, LBF, SORF, MORF, LORF, SIRF, MIRF, LIRF and N, respectively.

In this situation, 12 transfer fault diagnosis tasks can be formed by using the dataset to evaluate the DADAN, as displayed in TABLE II. The Gaussian noise is added into sample data of target domain to simulate transfer tasks under the actual working condition. The signal to noise ratio (SNR) is employed to assess the intensity of noise. Specifically, 2dB Gaussian noise is introduced into the target domain to enhance the domain gap, providing a more comprehensive evaluation of DADAN.

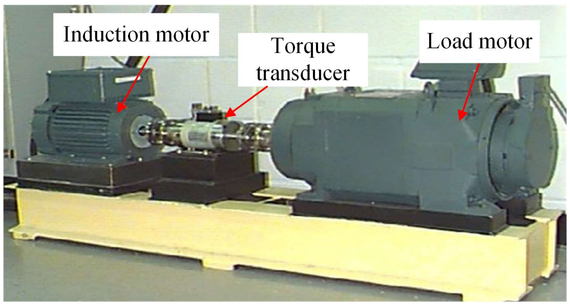

Fig. 6. The CWRU bearing fault test bench

TABLE II. The transfer tasks under the different working conditions.

Transfer case	Source domain	Target domain
$D_1 \to D_2$	0hp/1797rpm	1hp/1772rpm
$D_1 \to D_3$	0hp/1797rpm	2hp/1750rpm
$D_1 \to D_4$	0hp/1797rpm	3hp/1730rpm
$D_2 \to D_1$	1hp/1772rpm	0hp/1797rpm
$D_2 \to D_3$	1hp/1772rpm	2hp/1750rpm
$D_2 \to D_4$	1hp/1772rpm	3hp/1730rpm
$D_3 \to D_1$	2hp/1750rpm	0hp/1797rpm
$D_3 \to D_2$	2hp/1750rpm	1hp/1772rpm
$D_3 \to D_4$	2hp/1750rpm	3hp/1730rpm
$D_4 \to D_1$	3hp/1730rpm	0hp/1797rpm
$D_4 \to D_2$	3hp/1730rpm	1hp/1772rpm
$D_4 \to D_3$	3hp/1730rpm	2hp/1750rpm

The classification outcomes are displayed in TABLE III. The overall average accuracy of non-transfer learning method (CNN) is only 67.17%. However, the accuracy of CNN-MMD immediately increases to 90.34% as it adds MMD transfer loss. Hence, we infer that the transfer learning method is more meaningful in practical application of fault diagnosis due to it can align the domain boundary. Meanwhile, in terms of the precision of different approaches, it is evident that the overall mean precision of the DADAN approach achieves the best classification accuracy, yielding an average rate of 97.09%. Specifically, in 9 of the 12 transfer learning tasks, the DADAN shows the best performance. As illustrated in Fig. 7, compared with MCD-UDA and DL-ADAN, DADAN achieved superior performance for bearing fault diagnosis, which may be due to dual different architecture task-specific classifiers strategy of DADAN.

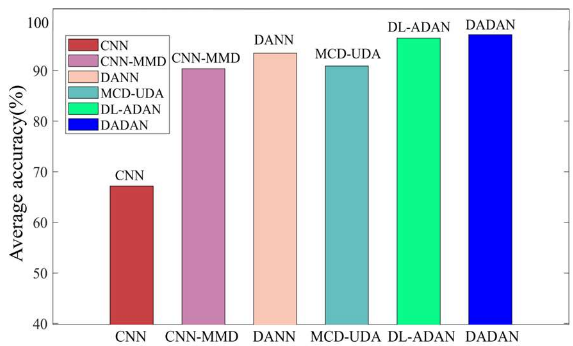

Fig. 7. The mean classification accuracy of the six methods.

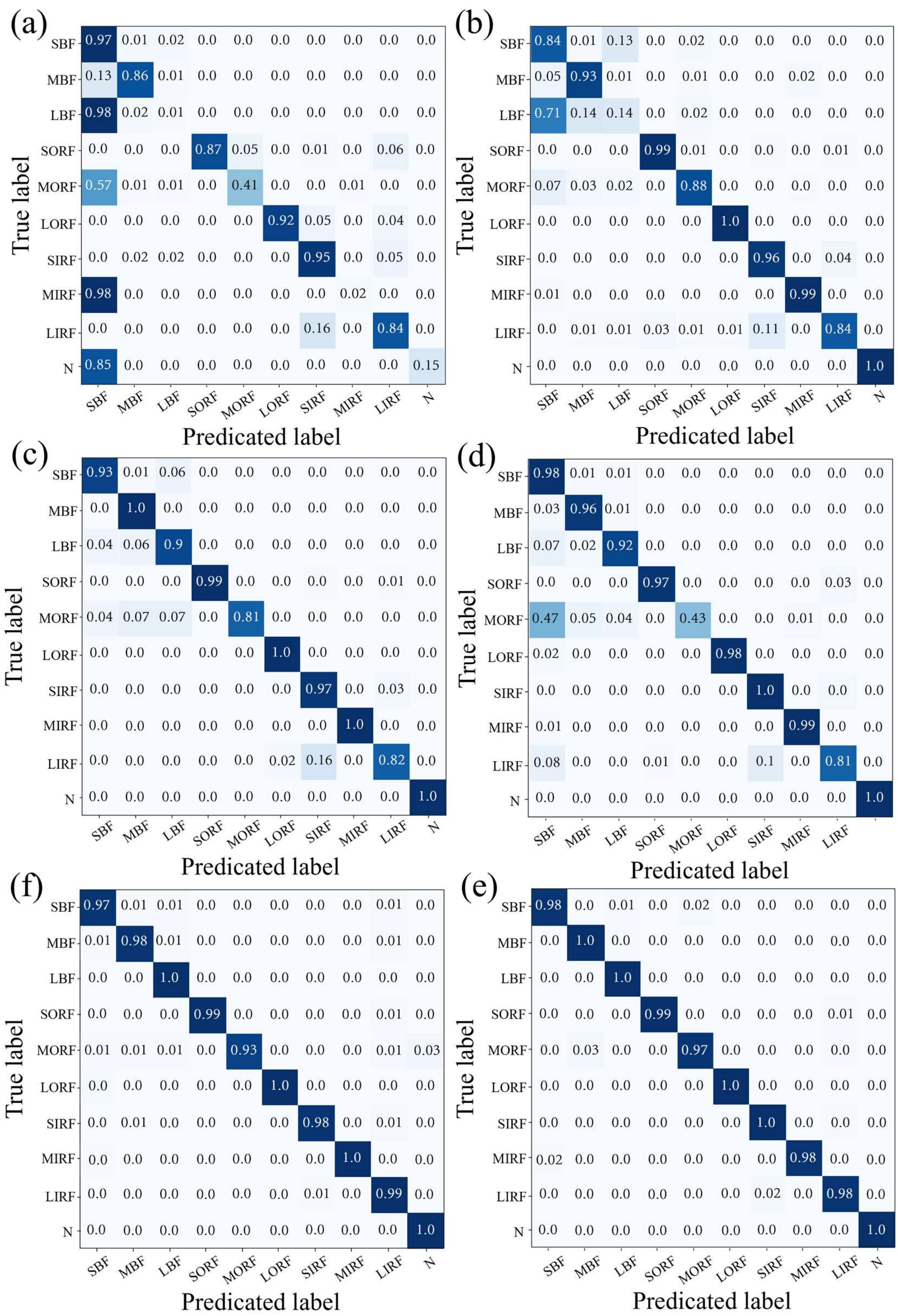

Fig. 8. Confusion matrices (%) on CWRU bearing fault platform diagnosis. (a)CNN, (b)CNN-MMD, (c)DANN, (d)MCD-UDA, (e)DL-ADAN, (f)The proposed DADAN

The confusion matrix of transfer task $D_2 \rightarrow D_1$ is selected for analysis, as demonstrated in Fig. 8. As illustrated in Fig. 8(a), for CNN, the accuracy of some categories is less than 30%, which greatly exposes the disadvantages of non-transfer learning. The classification accuracy of CNN-MMD is greatly improved, as demonstrated in Fig. 8(b). Interestingly, it is manifest that the overall performance of adversarial network domain adaptation methods, including DANN, MCD-UDA and DL-ADAN is relatively good. It can be found that most of the category accuracy obtained by the adversarial network domain adaptation methods is over 90%. However, the ball fault categories are misclassified by other methods, except for the proposed DADAN, as demonstrated in Fig. 8(c)-(e). Thanks to the unique strategy of the dual different classifiers and the feature center alignment across domain, the DADAN obtains substantially enhanced performance for diagnosis of ball fault with different sizes, as illustrated in Fig. 8(f). From the preceding discussion, it can be inferred that the proposed approach exhibits superior performance.

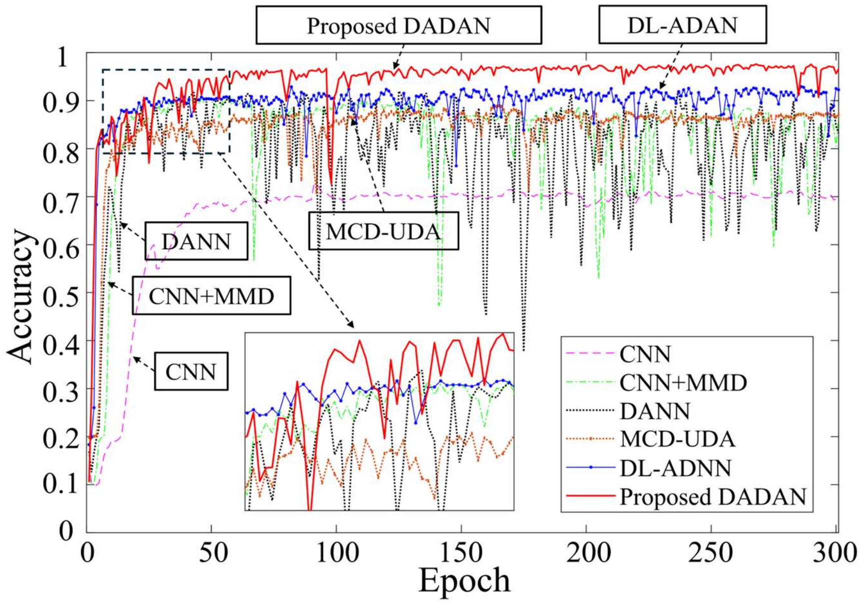

Fig. 9. Convergence performance of the six methods

TABLE III. Experimental results on CWRU bearing fault platform obtained by six models

Tasks	CNN	MMD CNN	DAN N	MCD-UDA	DL ADAN	Proposed DADAN
$D_1 \to D_2$	64.05	90.37	90.99	88.32	95.77	96.03
$D_1 \to D_3$	64.49	87.27	94.02	89.13	99.14	99.36
$D_1 \to D_4$	64.42	90.98	95.94	92.55	98.87	98.96
$D_2 \to D_1$	72.80	87.56	90.17	87.12	92.35	96.46
$D_2 \to D_3$	69.80	94.34	96.12	96.84	98.99	98.88
$D_2 \to D_4$	62.60	93.35	96.08	96.62	98.80	98.89
$D_3 \to D_1$	64.75	86.37	89.07	82.78	91.15	93.68
$D_3 \to D_2$	67.91	92.02	93.05	90.02	93.47	96.39
$D_3 \to D_4$	70.41	87.99	96.55	97.45	98.76	98.81
$D_4 \to D_1$	64.77	87.40	89.56	82.52	94.88	92.36
$D_4 \to D_2$	67.29	89.75	92.58	90.31	95.73	95.97
$D_4 \to D_3$	72.74	96.67	96.81	96.79	99.16	99.23
Averag	67.17	90.34	93.41	90.87	96.42	97.09

To further investigate the superiority of DADAN, the performance of the convergence curve of classification accuracy that reflects the stability and accuracy of the methods are employed for analysis. The convergence curves of task $D_2 \to D_1$ with different approaches are indicated in Fig. 9. Note that all the convergence curves are plotted using the original accuracy data points without any processing. Clearly, the convergence curves of the CNN-MMD and DANN show heavy fluctuations although they have fast convergence performance. The MCD-UDA, DL-ADNN and the proposed DADAN show better convergence performance, which can converge rapidly and show much better stability. Moreover, it is evident that DADAN shows superior classification accuracy. Therefore, it is not too difficult to spot that the proposed DADAN has the best convergence performance, showing its promising performance in the actual industry application.

Analogously, the t-SNE diagram of the task is presented for analysis, as demonstrated in Fig. 10. The various classes and domain information are distinguished using different colors. As visually demonstrated in Fig. 10(a), it is apparent that the distribution of features across domain of the CNN are out of alignment. Not surprisingly, the misalignment phenomenon of the CNN-MMD is comparatively alleviated as the MMD can align the embedded feature extracted by the CNN between the source and the target domain, as displayed in Fig. 10(b). Through visual inspection, we can find that the extracted features from the source and target domains are partially aligned for the DANN, UDA, DL-ADAN and the DADAN leveraging the domain adversarial learning process, as illustrated in Fig. 10(c)-(f). It should be pointed out that due to the large domain gap since 2dB noise is added into the target domain, the extracted feature by the MCD-UDA, the DL-ADAN and the DADAN are still not fully alignment. However, as indicated in Fig. 10(c)-(e), It is readily apparent that the fault feature of the ball fault in different size for the DANN, MCD-UDA and the DL-ADAN are hard to be separated in embedded feature space, which is consistent to fault diagnosis result displayed in Fig. 8(c)-(e), where the recognition accuracy of the ball fault with different size are relatively low. In contrast, we can find that the extracted feature by the DADAN has the clearest classification boundary. As visually demonstrated in Fig. 10(f), samples of the same category are clustered together, while samples of different categories are distinctly separated. Correspondingly, all the fault categories include the ball fault with different sizes are accurately detected by DADAN. According to the above analysis, it's not hard to see that the DADAN has best performance for bearing fault diagnosis.

Finally, the estimated feature representation across source and target domains for the transfer task $D_2 \to D_1$ is employed for visual analysis. During this process, the t-SNE is utilized to compress the dimensionality of the learned transferable features by the CNN feature extractor. Then we employ the kernel density estimation [38, 39] to fit the distribution of each component. The results of the above six methods are demonstrated in Fig.11- Fig.13. Clearly, we can find that the transferable features, such as Component 1 to Component 5, learned by CNN exhibit significant distribution divergence, as indicated in Fig. 11(a). After adding the MMD loss, the distribution discrepancy is a bit relieved, as indicated in Fig.11(b).

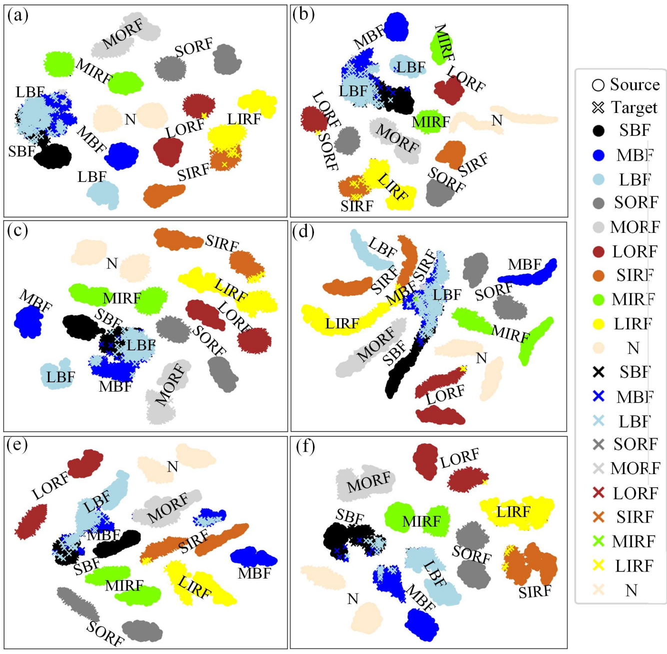

Fig.10 The t-SNE visualization of embedded features on the source and target domain, where the labels of 10 categories of bearing fault are marked from 1 to 10, respectively (a)CNN, (b)CNN-MMD, (c)DANN, (d)MCD-UDA, (e)DL-ADAN, (f)The proposed DADAN.

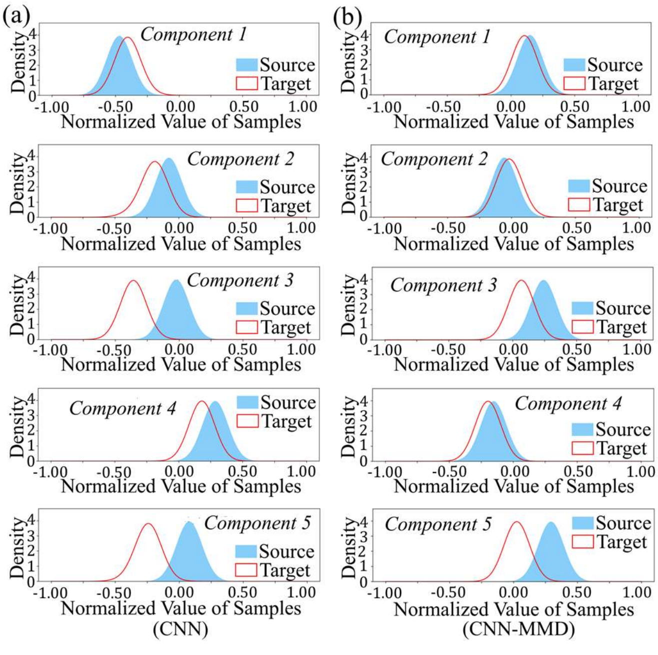

Fig.11. The estimated feature distribution between the source and target domain. (a)CNN, (b) CNN-MMD

For DANN, MCD-UDA, and DL-ADAN, the distribution discrepancy is diminished to a certain degree, as demonstrated in Fig. 12 and Fig. 13. However, some components still show serious distribution discrepancy. For example, the components 2 and 4 are seriously misaligned for the DL-ADAN, as illustrated in Fig.13 (a). On the contrary, we can find that the domain-wise feature discrepancy is greatly reduced by DADAN. where the five feature components are fully aligned, as demonstrated in Fig.13(b). The findings reveal that the proposed DADAN exhibits the best performance, which underlines the importance of the dual different classifiers structure and the discriminative feature center alignment across domain strategy.

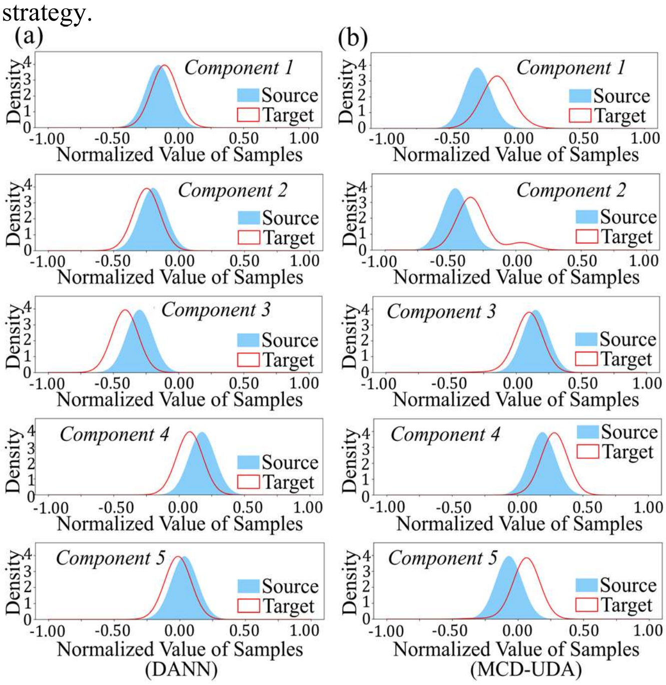

Fig.12. The estimated feature distribution between the source and target domain. (a)DANN, (b)MCD-UDA

D. Motor to brake bearing fault diagnosis analysis

To comprehensively assess performance and distinctive features of DADAN, supplementary cross-domain bearing fault diagnosis tests were conducted utilizing a customized experimental platform designed for this investigation. The challenging transfer fault diagnosis scenario can be tested on our own platform since it can stimulate the working conditions with large variation. Therefore, the superiority of DADAN can be revealed through the experimental platform. The test rig comprises a servo motor, a magnetic particle brake, a planetary gear system and the faulty bearing, as illustrated in Fig. 14. The servo motor is driven by a servo controller, supplying power to the test rig. The load is simulated using a magnetic powder brake. The planetary gear system operates with a reduction ratio of 3. The bearing fault signals are collected using the accelerometer under different load and rotational speed settings. Throughout the experiment, four typical operating conditions are considered as follows: (1) normal (N), (2) outer race fault (ORF), (3) inner race fault (IRF) and (4) roller fault (BF) with different defect sizes 0.5mm (S: small), 0.5mm (L: Large) artificially created using electrical discharge machining to replicate faults in rolling bearings (model: SKF6204). As illustrated in Fig. 12, the inner and outer race are designed with defect diameters of 1mm and 3mm, respectively. A triaxial piezoelectric acceleration sensor (PCB352C03) was implemented on the experimental apparatus. The drive system was scheduled to operate at incremental rotational velocities of 1247, 1338, 1428, and 1509 revolutions per minute, while torsional loading conditions were systematically applied at 0, 1.0, 1.5, and 2.0 N-meters respectively. The DAQ card (NI 9234) is utilized to acquire vibration data. Simultaneously, the acquisition frequency is adjusted to 2.56 kHz. The sample time is defined as 15 seconds.

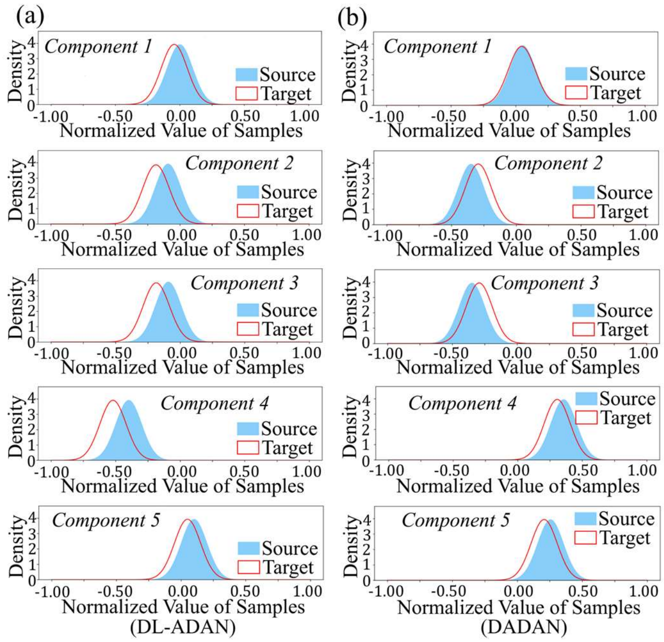

Fig. 13. The estimated feature distribution between the source and target domain (a)DL-ADAN, (b)The proposed DADAN.

The temporal waveforms of raw vibration signals corresponding to distinct defect states are presented in Figs. 15(a)-(c). The experimental dataset comprises four distinct operational states, each containing vibration signatures from bearings under three health status categories with divergent degradation levels. Consequently, the diagnostic effectiveness of the proposed methodology was rigorously examined through the systematic implementation of twelve differentiated test scenarios. There are 6 categories of bearing fault, which are labeled as N, LBF, SIRF, LIRF, SORF, LORF, respectively.

The transfer tasks along with their respective operating conditions are detailed in TABLE IV. In this context, $D_1 \to D_2$ signifies a transfer learning scenario where data is adapted from the source domain D_1 to the target domain D_2. It is worth mentioning that 10 dB of noise is introduced into the target domain dataset to increase the domain bias.

TABLE IV. The transfer tasks under the different working conditions

Scenario	Source	Target
$D_2 \to D_1$	1149 rpm/0 Nm	1338 rpm/1.5 Nm
$D_3 \to D_4$	1149 rpm/1Nm	1338 rpm/2 Nm
$D_5 \to D_6$	1247 rpm/0 Nm	1428 rpm/1.5Nm
$D_7 \to D_8$	1247 rpm/1 Nm	1428 rpm/2 Nm
$D_9 \to D_{10}$	1338 rpm/0 Nm	1598 rpm/1.5Nm
$D_{11} \to D_{12}$	1338 rpm/1 Nm	1598 rpm/2Nm
$D_2 \to D_1$	1338rpm/1.5 Nm	1149 rpm/0 Nm
$D_4 \to D_3$	1338 rpm/2 Nm	1149 rpm/1Nm
$D_6 \to D_5$	1428 rpm/1.5Nm	1247 rpm/0 Nm
$D_8 \to D_7$	1428 rpm/2 Nm	1247 rpm/1 Nm
$D_{10} \to D_9$	1598 rpm/1.5Nm	1338 rpm/0 Nm
$D_{12} \to D_{11}$	1598 rpm/2Nm	1338 rpm/1 Nm

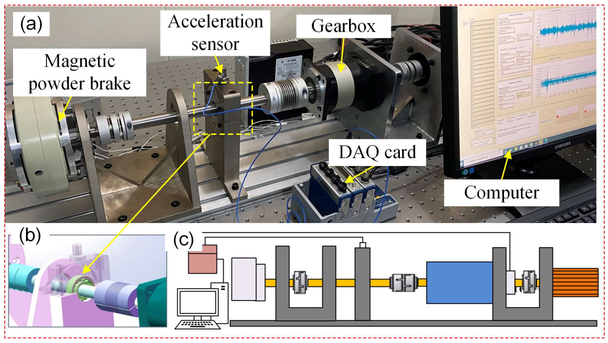

Fig. 14. The test rig for bearing fault diagnosis. (a) The physical map of the designed bearing fault test rig, (b) The model map of the tested bearing, (c) The schematic diagram of test rig.

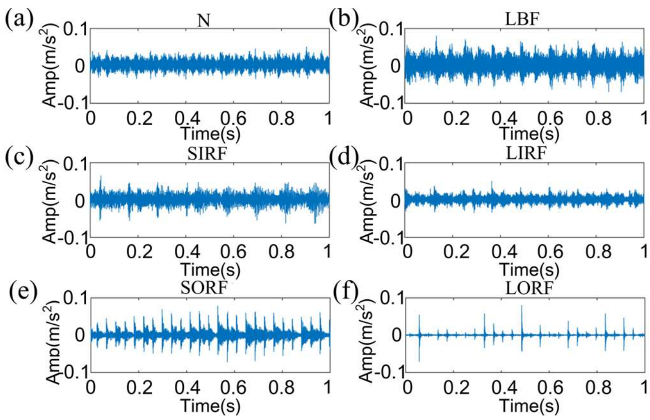

Fig.15.The original signal collected from the bearing fault test rig. (a) N, (b)LBF, (c)SIRF, (d)LIRF, (e)SORF, (f)LORF

As demonstrated in TABLE V, we present the classification outcomes on the tested bearing fault set of target domain by six different methods. The classification accuracy across target domain is computed by averaging the results from three iterations, where the average values are employed for comparison. Clearly, several conclusions can be drawn. Firstly, domain adaptation is the crucial procedure for addressing the fault diagnosis scenario under changing operational environments. For instance, the overall mean precision of CNN without transfer learning is merely 52.58%. However, after adding MMD transfer loss, the accuracy of CNN-MMD immediately increases to 79.37%. Secondly, it can be observed that there are significant performance gaps between CNN-MMD and adversarial learning approaches like DANN, DL-ADNN, and DADAN. Generative adversarial networks exhibit superior holistic performance compared to CNN-MMD methodology in cross-domain fault recognition tasks. Thirdly, it can be found DADAN achieves the highest classification accuracy among all evaluated approaches, in which the overall classification accuracy of DADAN is the highest. Furthermore, it is observable that the average classification accuracy of DADAN attains 98.34%, which is higher than MCD-UDA and DL-ADADN by 10.39% and 3.91% respectively, indicating the superior performance of DADAN, as described in Fig.16.

Nonetheless, it should be noting that a bit serious misclassification phenomenon occurred in some small minority transfer path such as $D_2 \to D_1$ and $D_3 \to D_4$ for the DANN, MCD-UDA and DL-ADAN, which may attribute the wrong alignment across domains. The inner fault signal with a 1mm crack is relatively weak. It becomes even weaker after the addition of Gaussian white noise. Consequently, the signal patterns of inner race defects and normal conditions in both the source and target domains tend to exhibit highly comparable characteristics, which lead to the wrong alignment across domains in the embedded feature space. The MCD-UDA and DL-ADAN consist of two adversarial frameworks, each equipped with dual neural network classifiers of same structure, which may generate similar decision boundaries. Thus, the task-specific boundaries obtained by MCD-UDA and the DL-ADAN may be not the ideal ones for recognizing the fault type. The proposed DADAN shown improvement for this problem since the different dual structure classifiers are employed, which can obtain better task-specific boundaries for classifying the fault type in target domain.

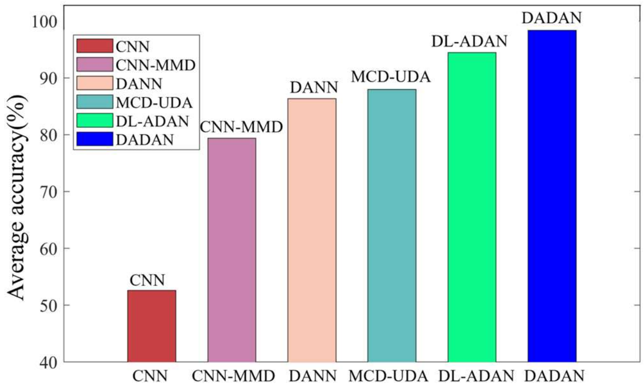

Fig. 16. The average classification accuracy of all methods.

TABLE V. Experimental results on our own test rig of six methods

Tasks	CNN	MMD-CNN	DANN	MCD-UDA	DL-ADAN	Proposed DADAN
$D_2 \to D_1$	38.72	82.11	69.22	82.83	96.89	99.89
$D_3 \to D_4$	28.78	80.33	89.70	82.51	96.50	99.94
$D_5 \to D_6$	55.39	94.72	96.72	92.55	99.33	99.67
$D_7 \to D_8$	28.78	91.72	96.66	93.61	98.39	100.00
$D_9 \to D_{10}$	53.61	80.56	98.5	96.50	96.33	100.00
$D_{11} \to D_{12}$	57.94	94.50	94.22	95.72	99.83	100.00
$D_2 \to D_1$	53.83	52.44	50.00	85.27	83.25	89.06
$D_4 \to D_3$	69.39	88.56	85.33	77.11	88.56	99.22
$D_6 \to D_5$	61.69	93.72	88.11	72.89	99.94	95.17
$D_8 \to D_7$	77.39	58.17	80.89	89.33	100	99.22
$D_{10} \to D_9$	37.79	44.94	93.94	90.56	83.06	98.01
$D_{12} \to D_{11}$	67.61	90.72	99.72	99.83	99.89	99.89
Average	52.58	79.37	86.35	87.95	94.43	98.34

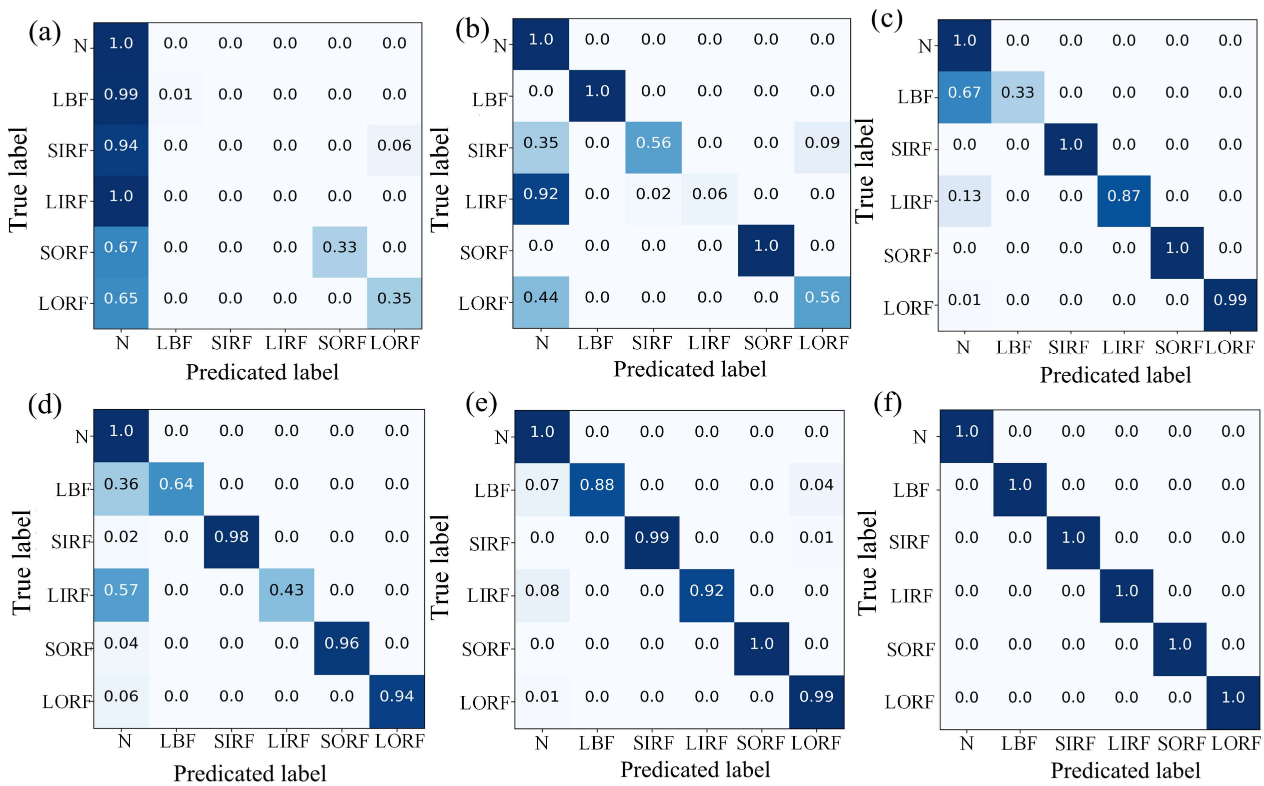

Fig.17. Confusion matrices (%) on our own test rig. (a)CNN, (b)CNN-MMD, (c)DANN, (d)MCD-UDA, (e)DL-ADAN, (f) DADAN

In addition, the confusion matrix of task $D_3 \rightarrow D_4$ is selected for specific analysis, as illustrated in Fig. 17. Due to the considerable distribution disparity across domains. the traditional CNN, lacking transfer learning capability, significantly misclassifies these target domain samples, as illustrated in Fig. 17(a). For example, the normal data are wrongly classified into the inner fault and outer fault data. When feature-based transfer loss MMD is added to CNN, the classification accuracy is greatly improved, as illustrated in Fig. 17(b). The DANN and MCD-UDA show better performance than the CNN-MMD while it is inferior than DL-DANN, as indicated in Fig. 17(c)-(f). Relative to the recently published DL-DANN, the proposed method demonstrates an advantage to some extent. As illustrated in Fig. 17(f), the proposed DL-DANN achieves exceptional classification performance, attaining 100% recognition accuracy across all categories for the unsupervised transfer learning scenarios involving target domain data, which may be attributed to the strategy of dual classifier with different structures of the proposed method, verifying the motivation of this work. Finally, the results of the accuracy convergence curve of the task $D_3 \rightarrow D_4$ are plotted in Fig 18. The convergence performance of the classical CNN is less effective regarding the classification accuracy since it has no transfer learning ability, indicating that traditional CNN is uncapable of dealing with the transfer tasks with large domain bias.

Compared with CNN, the convergence performance of CNN-MMD shows great improvement in terms of classification accuracy since MMD loss is added to realize the feature transfer learning across domains. However, it shows great oscillation during the convergence process. Similar phenomenon can be observed for DANN and MCD-UDA. Meanwhile, we can find that DL-ADNN achieves relatively better convergence performance. It can converge rapidly although stability leaves much to be desired. On the whole, with embedded feature center alignment across domain and the dual different classifiers strategy, DADAN enjoys much faster and stably convergence performance compared with MCD-UDA and DL-DANN. The results illustrate the role of dual classifiers with different structures and deep cluster alignment in maintaining stability and enhancing the diagnostic effectiveness of DADAN.

Furthermore, the t-SNE technique is employed to visualize the features, which can demonstrate the domain adaptability of all the methods. Similarly, the transfer task with the path $D_3 \rightarrow D_4$ is selected to plot the t-SNE diagram, as illustrated in Fig.19, where various colors denote different categories while different dots shapes represent different domains. The latent embedded features such as Component 1 to Component 4 of the source and the target domain learned by the classical CNN without transfer learning ability are totally mismatched, as illustrated in Fig.19(a). Meanwhile, with feature alignment by MMD, CNN-MMD can realize partial alignment of embedded feature across domains. However, the fault categories in target domain are inseparable, as displayed in Fig.19(b). As a result, some misclassifications occurred using CNN and CNN-MMD. For the DANN, the fault classes show clear separation while the embedded feature across domains are not well aligned. As a result, DANN method with only one classifier is not able to discern the clear boundary in the target domain, as displayed in Fig.19(c). Embedded feature across domains gained by MCD-UDA and DL-ADNN show the similar pattern with the DANN. However, the performance of MCD-UDA and DL-ADNN are better than DANN in terms of classification accuracy, which may attribute the dual classifiers adopted by them, as illustrated in Fig.19(d)-(e). Owing to the feature center alignment strategy, the embedded feature learned by the proposed DADAN across domain are well matched and aligned, which is facilitating for gaining the optimal decision boundaries. Meanwhile, thanks to the tactic of dual different classifiers, the same fault category is clearly gathered while different fault classes are well separated in the embedded feature, as illustrated in Fig.17(f). The well alignment of the feature across domains and the clear separations indicate that the DADAN can well identify the boundaries between different classes, which further affirm the superiority of DADAN.

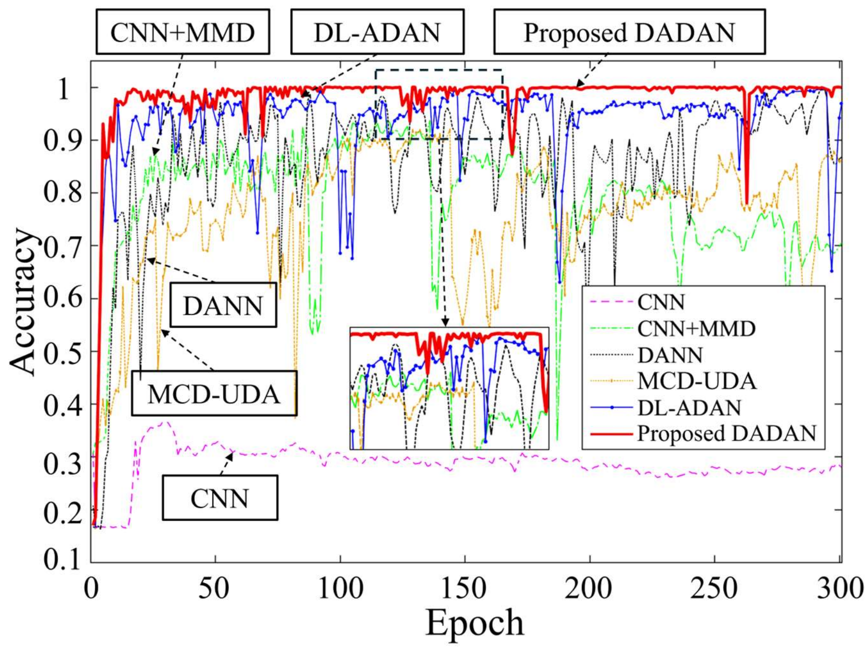

Fig. 18. Convergence performance of the six methods

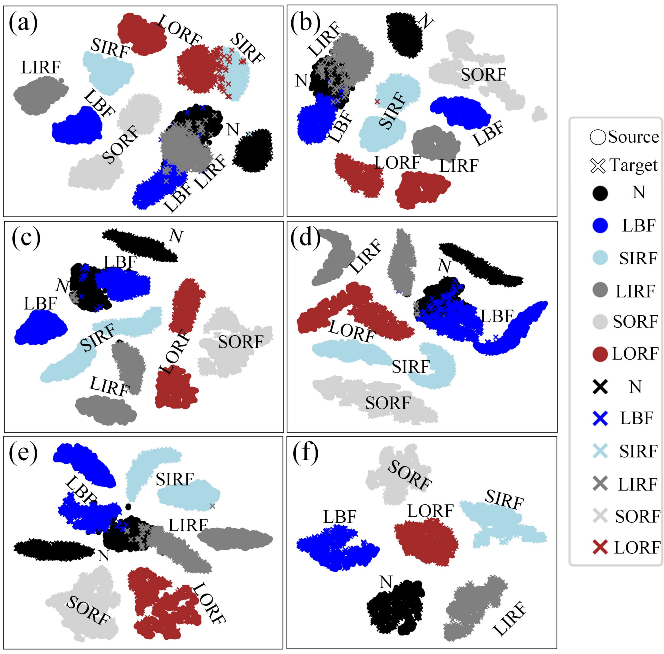

Fig. 19. The t-SNE visualization of embedded features on the source and target domain, where the labels of 6 categories of bearing fault are marked from 1 to 6, respectively (a) CNN, (b)CNN-MMD (c)DANN, (d)MCD-UDA, (e)DL-ADAN, (f)The proposed DADAN

From another perspective, the kernel density estimation technique is utilized to harmonize the feature distributions across two domains. We plot the results of the above six methods, as illustrated in Fig.20, Fig.21 and Fig.22.

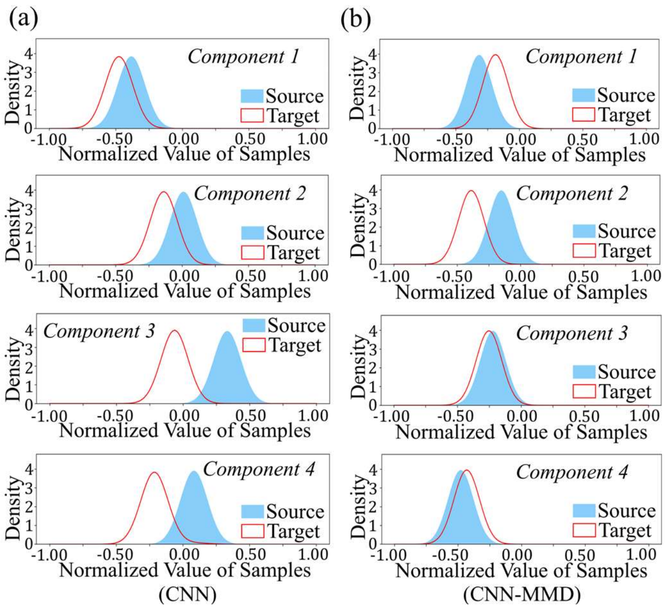

Fig. 20. The estimated feature distribution between the source and target domain (a)CNN, (b)CNN-MMD

Similarly, the disparity in the distribution divergence of transferable features extracted by CNN is notably significant, as indicated in Fig.20(a), indicating the poor transfer learning ability of CNN, especially for dealing with the transfer tasks with large domain shift. The distribution discrepancy is reduced for CNN-MMD, since MMD loss can enhance the domain adaptation ability, as indicated in Fig.20(b).

Simultaneously, the proposed DANN demonstrates a significant mitigation of the feature distribution gap is diminished between domains. However, the performance of DANN shows degradation if we compared it with the MCD-UDA and DL-DANN, as illustrated in Fig.21. Moreover, as indicated in Fig.22(b), the proposed DADAN improves the feature distribution alignment greatly as compared with MCD-UDA and DL-ADNN, since the kernel density components related to the embedded fault feature are fully matched across domains of the proposed DADAN. Hence, it can be found that DADAN has the most superior performance.

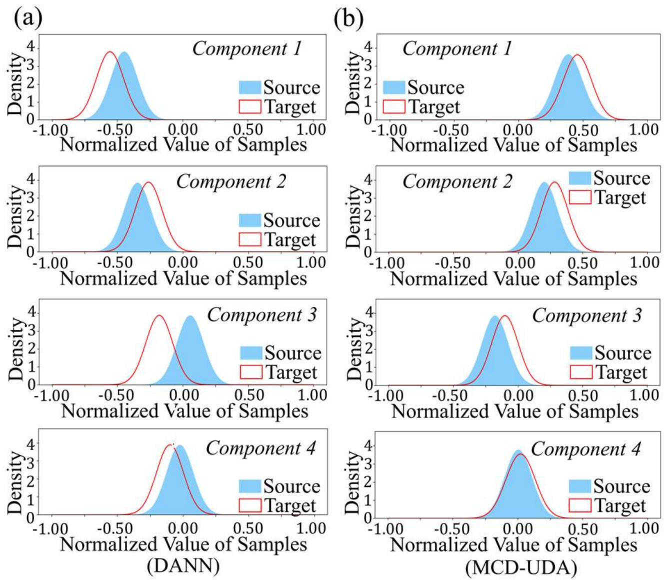

Fig. 21. The estimated feature distribution between the source and target domain (a)DANN, (b)MCD-UDA

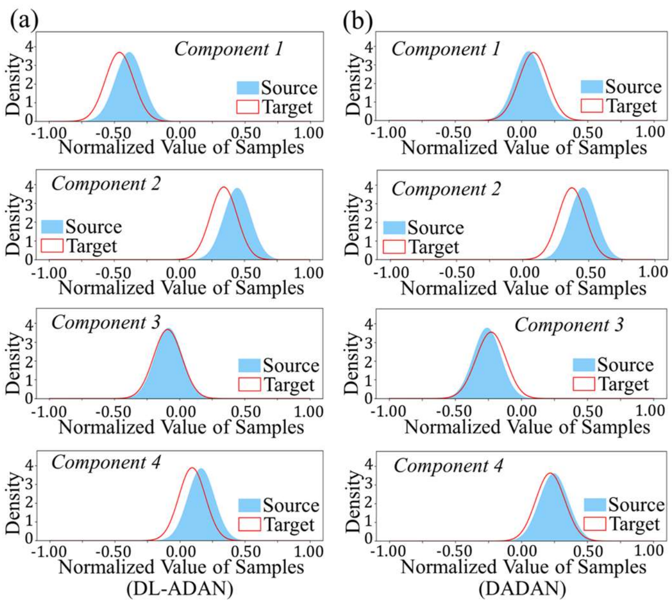

Fig. 22. The estimated feature distribution between the source and target domain (a)DL-ADAN, (b)The proposed DADAN method

V. Conclusions

This paper introduces an unsupervised DADAN approach for diagnosing bearing faults across different operating conditions. The advancements of this research can be outlined as follows: 1) The DADAN combines adversarial learning with feature center alignment to assist in the extraction of embedded invariant features across domains, which can augment the domain adaptation ability. 2) The dual classifiers with different structures can obtain better classification boundaries in target domain. 3) The feature center alignment across domain can facilitate extraction of domain-invariant features and alignment of classes across domains. With the above strategies, the proposed method exhibits excellent performance for diagnosis transfer of learning tasks with large domain shift relative to alternative domain adaptation approaches.

A series of comprehensive experiments are conducted on two representative fault datasets across multiple transfer scenarios to validate the effectiveness and benefits of DADAN, indicating that it is a robust and powerful method for fault diagnosis under diverse working environments in industrial applications.

REFERENCES

[1] M. Alabsi, Y. Liao, and A. A. Nabulsi, "Bearing fault diagnosis using deep learning techniques coupled with handcrafted feature extraction: A comparative study," J. Vib. Control, vol. 27, no. 3-4, pp. 404-414, 2021

[2] L. Xu, S. Chatterton, and P. Pennacchi, "Rolling element bearing diagnosis based on singular value decomposition and composite squared envelope spectrum," Mech. Syst. Signal Process, vol. 148, p. 107174, 2021.

[3] K. Zheng, T. Li, Z. Su, and B. Zhang, "Sparse elitist group lasso denoising in frequency domain for bearing fault diagnosis," IEEE Trans. Ind. Inform., vol. 17, no. 7, pp. 4681-4691, 2020.

[4] Y Lei, B Yang, X Jiang, F Jia, N Li, and AK Nandi, "Applications of machine learning to machine fault diagnosis: A review and roadmap," Mechanical Systems and Signal Processing, vol. 138, p. 106587, 2020.

[5] G Yang, and X Liu, "Study on Method of Bearing Fault Detection Based on Vibration Signal Analysis," Engineering Letters, vol. 31, no.3, pp1009-1015, 2023.

[6] K Zheng, D Yao, Y Shi, B Wei, D Yang, and B Zhang, "An adaptive group sparse feature decomposition method in frequency domain for rolling bearing fault diagnosis," ISA Transactions, vol. 138, pp. 562-581, 2023.

[7] R Jegadeesh Waran and V Sugumaran, "Fault diagnosis of automobile hydraulic brake system using statistical features and support vector machines," Mechanical Systems and Signal Processing, vol. 52, pp. 436-446, 2015.

[8] BS Yang, X Di, and T Han, "Random forests classifier for machine fault diagnosis," Journal of Mechanical Science and Technology, vol. 22, no. 9, pp. 1716-1725, 2008.

[9] P Jayaswal, SN Verma, and AK Wadhwani, "Development of EBP-Artificial neural network expert system for rolling element bearing fault diagnosis," Journal of Vibration and Control, vol. 17, no. 8, pp. 1131-1148, 2011.

[10] Z He, C Shen, B Chen, J Shi, W Huang, Z Zhu, and Wang, "A new feature boosting based continual learning method for bearing fault diagnosis with incremental fault types," Advanced Engineering Informatics, vol. 61, p. 102469, 2024.

[11] D. Li, Y. Yang, S. Shen, J. He, H. Shen, Q. Yue, S. Hong, and F. Deng, “Research on Fault Diagnosis based on Improved Generative Adversarial Network under Small Samples,” IAENG International Journal of Computer Science, vol. 50, no. 1, pp. 7-13, 2023.

[12] R Zhao, R Yan, Z Chen, K Mao, and P Wang, "Deep learning and its applications to machine health monitoring," Mechanical Systems and Signal Processing, vol. 115, pp. 213-237, 2019.

[13] S Haidong, J Hongkai, and L Xingqiu, "Intelligent fault diagnosis of rolling bearing using deep wavelet auto-encoder with extreme learning machine," Knowledge-Based Systems, vol. 140, pp. 1-14, 2018

[14] Y Zhang, T Zhou, X Huang, L Cao, and Q Zhou, "Fault diagnosis of rotating machinery based on recurrent neural networks," Measurement, vol. 171, p. 108774, 2021.

[15] W Lu, B Liang, Y Cheng, and D Meng, "Deep model-based domain adaptation for fault diagnosis," IEEE Transactions on Industrial Electronics, vol. 64, no. 3, pp. 2296-2305, 2016.

[16] M Azamfar, X Li, and J Lee, "Intelligent ball screw fault diagnosis using a deep domain adaptation methodology," Mechanism and Machine Theory, vol. 151, p. 103932, 2020.

[17] J Tian, D Han, H Karimi, Y Zhang, and P Shi, "A universal multi-source domain adaptation method with unsupervised clustering for mechanical fault diagnosis under incomplete data," Neural Networks, vol. 173, p. 106167, 2024.

[18] B Sun, J Feng, and K Saenko, "Return of frustratingly easy domain adaptation," Proceedings of the AAAI Conference on Artificial Intelligence, vol. 30, no. 1, pp. 2058-2065, 2016.

[19] KM Borgwardt, A Gretton, MJ Rasch, and HP Kriegel, "Integrating structured biological data by kernel maximum mean discrepancy," Bioinformatics, vol. 22, no. 14, pp. e49-e57, 2006.

[20] J Cheng, R Liang, Z Liang, and L Zhao, "A Deep Adaptation Network for Speech Enhancement: Combining a Relativistic Discriminator With Multi-Kernel Maximum Mean Discrepancy," IEEE/ACM Transactions on Audio, Speech, and Language Processing, vol. 29, pp. 41-53, 2020.

[21] B Sun and K Saenko, "Deep CORAL: Correlation Alignment for Deep Domain Adaptation," in Computer Vision - ECCV 2016 Workshops, 2016, vol. 9915, ISBN: 978-3-319-49408-1

[22] R Li, S Li, K Xu, J Lu, G Teng, and J Du, "Deep domain adaptation with adversarial idea and coral alignment for transfer fault diagnosis of rolling bearing," Measurement Science and Technology, vol. 32, no. 9, p. 094009, 2021.

[23] Y. Ganin, E. Ustinova, H. Ajakan, P. Germain, H. Larochelle, F. Laviolette, M. Marchand, and V. Lempitsky, "Domain-adversarial training of neural networks," J. Mach. Learn. Res., vol. 17, no. 1, pp. 2096-2030, 2016

[24] T Han, C Liu, W Yang, and D Jiang, "A novel adversarial learning framework in deep convolutional neural network for intelligent diagnosis of mechanical faults," Knowledge-Based Systems, vol. 165, pp. 474-487, 2019.

[25] Z Chai and C Zhao, "A fine-grained adversarial network method for cross-domain industrial fault diagnosis," IEEE Transactions on Automation Science and Engineering, vol. 17, no. 3, pp. 1432-1442, 2020.

[26] S Asutkar and S Tallur, "Deep transfer learning strategy for efficient domain generalization in machine fault diagnosis," Scientific Reports, vol. 13, p. 6607, 2023.

[27] Y Qin, Q Yao, Y Wang, and Y Mao, "Parameter sharing adversarial domain adaptation networks for fault transfer diagnosis of planetary gearboxes," Mechanical Systems and Signal Processing, vol. 160, p. 107936, 2021.

[28] K Saito, K Watanabe, and Y Ushiku, "Maximum classifier discrepancy for unsupervised domain adaptation," in Proceedings of the IEEE Conference on Computer Vision and Pattern Recognition (CVPR), 2018, pp. 3723-3732.

[29] Z Wu, H Jiang, T Lu, and K Zhao, "A deep transfer maximum classifier discrepancy method for rolling bearing fault diagnosis under few labeled data," Knowledge-Based Systems, vol. 196, p. 105814, 2020.

[30] J Jiao, J Lin, M Zhao, and K Liang, "Double-level adversarial domain adaptation network for intelligent fault diagnosis," Knowledge-Based Systems, vol. 205, p. 106236, 2020.

[31] J Snell, K Swersky, and RS Zemel, "Prototypical networks for few-shot learning," in Proceedings of the 31st International Conference on Neural Information Processing Systems (NIPS'17), Curran Associates Inc., Red Hook, NY, USA, pp. 4080-4090, 2017

[32] T. Jing and Z. Ding, "Adversarial Dual Distinct Classifiers for Unsupervised Domain Adaptation," *2021 IEEE Winter Conference on Applications of Computer Vision (WACV)*, Waikoloa, HI, USA, 2021, pp. 605-614,

[33] H. Tang, K. Chen and K. Jia, "Unsupervised Domain Adaptation via

Structurally Regularized Deep Clustering," 2020 IEEE/CVF Conference on Computer Vision and Pattern Recognition (CVPR), Seattle, WA, USA, 2020, pp. 8722-8732,

[34] WA Smith and RB Randall, "Rolling element bearing diagnostics using the Case Western Reserve University data: A benchmark study," Mechanical Systems and Signal Processing, vol. 64, pp. 100-131, 2015.

[35] S Ma, G Cheng, Y Li, and RZ Zhao, "Dimension reduction method of high-dimensional fault datasets based on C_M_t-SNE under unsupervised background," Measurement, vol. 214, p. 112835, 2023.

[36] B Yang, Y Lei, F Jia, N Li, and Z Du, "A Polynomial Kernel Induced Distance Metric to Improve Deep Transfer Learning for Fault Diagnosis of Machines," IEEE Transactions on Industrial Electronics, vol. 67, no. 11, pp. 9747-9757, 2019.

[37] L Guo, Y Lei, S Xing, T Yan, and N Li, "Deep convolutional transfer learning network: A new method for intelligent fault diagnosis of machines with unlabeled data," IEEE Transactions on Industrial Electronics, vol. 66, no. 9, pp. 7316-7325, 2018.

[38] J Zhu, N Chen, and C Shen, "A New Deep Transfer Learning Method for Bearing Fault Diagnosis Under Different Working Conditions," IEEE Sensors Journal, vol. 20, no. 15, pp. 8394-8402, 2019.

[39] Z Wang, Z Su, Y Deng, J Kurths, and J Wu, "Spatial network disintegration based on kernel density estimation," Reliability Engineering & System Safety, vol. 245, p. 110005, 2024.